

PAPER • OPEN ACCESS

## Photocatalytic Degradation of Organic Pollutant using Visible Active - Boron Doped Photocatalyst

To cite this article: Md Noor Bin Arifin *et al* 2021 *IOP Conf. Ser.: Mater. Sci. Eng.* **1092** 012062

View the [article online](#) for updates and enhancements.

### You may also like

- [Improving oleophobicity and hydrophilicity of superhydrophobic surface by TiO<sub>2</sub>-based coatings](#)  
Marzieh Sadat Hosseini, Mohammad Taghi Sadeghi and Masoud khazaei
- [In situ synthesis of TiO<sub>2</sub>\(B\) nanotube/nanoparticle composite anode materials for lithium ion batteries](#)  
Xiang Liu, Qian Sun, Alan M C Ng et al.
- [Nanoscale water spray assisted synthesis of CAs@B-TiO<sub>2</sub> core-shell nanospheres with enhanced visible-light photocatalytic activity](#)  
Hengcheng Wan, Ling Zhang, Yi Li et al.



The Electrochemical Society  
Advancing solid state & electrochemical science & technology

242nd ECS Meeting

Oct 9 – 13, 2022 • Atlanta, GA, US

Abstract submission deadline: **April 8, 2022**

Connect. Engage. Champion. Empower. Accelerate.

**MOVE SCIENCE FORWARD**



Submit your abstract



# Photocatalytic Degradation of Organic Pollutant using Visible Active - Boron Doped Photocatalyst

Md Noor Bin Arifin<sup>1</sup>, Mostafa Tarek<sup>1</sup>, Maksudur Khan,<sup>2,3</sup>

<sup>1</sup>Faculty of Chemical Engineering Technology and Process, Universiti Malaysia Pahang, Lebuhraya Tun Razak, 26300 Gambang, Kuantan, Pahang, Malaysia

<sup>2</sup>College of Engineering, Universiti Malaysia Pahang, Lebuhraya Tun Razak, 26300 Gambang, Kuantan, Pahang, Malaysia

<sup>3</sup>Centre of Excellence for Advanced Research in Fluid Flow, Universiti Malaysia Pahang, Lebuhraya Tun Razak, 26300 Gambang Kuantan, Pahang, Malaysia

Email: noormd@ump.edu.my

**Abstract.** Boron-doped TiO<sub>2</sub> (B-TiO<sub>2</sub>) nanocatalysts were prepared by the sol-gel method, characterized by X-Ray diffraction (XRD) and diffuse reflectance UV-vis spectroscopy (DRS). XRD results exhibited that the doping of boron element could potentially inhibit the growth of grain and promote the formation of anatase phase and diboron trioxide phase. The photocatalytic activity of the B-TiO<sub>2</sub> nanophotocatalyst was evaluated by the degradation test on one of the most widely used organic dyes, methylene blue (MB). The result indicated the doped B-TiO<sub>2</sub>, with 0.25g/L catalyst loading, were more active than the undoped TiO<sub>2</sub> in breaking down the MB. The maximum conversion of MB by the doped TiO<sub>2</sub> was 80.60%, approximately 14% higher than the pristine TiO<sub>2</sub>. The as-synthesized B-TiO<sub>2</sub> was calcined at 450°C demonstrated higher photocatalytic activity than undoped TiO<sub>2</sub> after 240mins of visible light illumination.

## 1. Introduction

The escalating crises in energy and environment pose a new challenge to the social and economic development at a global scale. Hence the most researched and explored semiconductor photocatalyst, TiO<sub>2</sub> offers the virtues of low cost, highly efficient, renewable, low toxic and highly stable for the application in wastewater treatment and energy conservation [1]–[6]. TiO<sub>2</sub> has become the most extensively studied metal oxide semiconductors owing to its special optical, physical and photochemical properties. Nevertheless, TiO<sub>2</sub> suffers from a few drawbacks, for instance rapid recombination of photoinduced species, limited charge transfer and narrow absorption of solar spectrum which hamper its further application [7]–[9].

There have been numerous efforts to address the abovementioned issues such as the optimization of the phase junction via semiconductor coupling. Among the successful coupling strategies are having binary semiconductors; TiO<sub>2</sub>/MgO, TiO<sub>2</sub>/CuO, TiO<sub>2</sub>/ZrO<sub>2</sub>, TiO<sub>2</sub>/ZnO synthesized and employed in the application of organic pollutants decomposition, carbon dioxide reduction and hydrogen production [1–4]. One way to modulate the properties of highly active catalysts is by doping, through which the intrinsic band structures and optical properties can be tuned and improved [5–8]. This approach can be achieved either by employing metal or non-metal elements. Based on the reports in the literatures [6][9], the former demonstrated inevitable defects namely high numbers of electron-hole (e<sup>-</sup> - h<sup>+</sup>) pairs recombination centers, low thermal stability and photocorrosion potential. On the other hands, among the non-metal doping agents (O, S, C, N, B etc.), boron has already been substantiated to mitigate the properties of TiO<sub>2</sub> through the modulation of band gap structure and charge transfer efficiency [10,11].



The aim of the investigation reported here was to characterize the as-prepared boron doped TiO<sub>2</sub> using XRD and UV-vis DRS, after which the photocatalytic activity test was conducted and the performance was evaluated by irradiating thiazine molecules, methylene blue under the visible light source. The first section of this paper, Section 2 presents the overall progress on the photoremediation work on organic pollutants and the types of photocatalysts that have been employed to break down the recalcitrant molecules. In Section 3, the preparation method elaborates on the technique used to synthesize boron doped TiO<sub>2</sub> using sol-gel method. The discussion of the results in this work is presented in Section 4 where XRD and UV-vis diffusive reflectance (DRS) analysis were done. The characterization was performed to confirm the characteristic crystalline phase and band gap of the as-synthesized photocatalysts, from the undoped catalysts. The photocatalytic activity was then conducted to test the efficiency of the synthesized catalyst at fixed catalyst loading.

## 2. Methods

### 2.1. Synthesis of Boron Doped TiO<sub>2</sub>

The synthesis of TiO<sub>2</sub> and B-TiO<sub>2</sub> catalysts was conducted by emulating a previously reported work [21]. In this sol-gel technique, a precursor solution was initially prepared through the dilution of boric acid in 10 mL anhydrous ethanol (99.5%). The mixture was then added with the 4.2 mL tert-butyl titanate (Sigma-Aldrich, 97%), and pH adjustment was done with glacial acetic acid (Merck) to achieve a pH value in the range of 3-4 and the solution is continuously stirred for 30 mins. Then, 20 mL ethanol was poured into the precursor solution and stirred for two more hours. Next, ammonia aqueous solution (Sigma-Aldrich, 35%) was added drop wise until the pH is 9. Repeating the previous step, another addition of 10 mL ethanol into the basic solution was required whilst maintaining the stirring for another 30 mins. The suspension was centrifuged and washed five times. The resulting solid was dried at 60 °C overnight, manually grinded and finally calcined at 450 °C for 30 mins.

### 2.2. Characterization of Boron Doped TiO<sub>2</sub>

For the characterization part, X-ray diffraction (XRD) and diffusive reflectance UV-Vis spectroscopy were employed to analyse the properties of boron doped TiO<sub>2</sub> and the undoped TiO<sub>2</sub>. The XRD patterns were obtained at room temperature using Rigaku MiniFlex II at Bragg angle of  $2\theta = 3-80^\circ$  with a scan step of 0.02 °/min for the sample powders. The measurements were performed at 30 kV and 15 mA using Cu-K $\alpha$  emission and a nickel filter. The angles of coherent were calculated by using Bragg's law [22], [23] as follows:

$$2d \sin \theta = n\lambda \quad (1)$$

where,  $\theta$  and  $d$  are the scattering angle and inter planar distance of the crystalline solid,  $n$  is a positive integer and  $\lambda$  is the wavelength of incident wave. The UV-vis spectroscopy of the as-prepared catalysts were performed at the wavelength range of 220-900 nm. The spectrophotometer, model Shimadzu UV 2600 UV-Vis was employed to determine the absorbance of dyes, from which the band gap energy was determined. Band gap energy was calculated from the required wavelengths to make the photocatalysts active according to the following Eq. (2) [24]:

$$\text{Band gap of semiconductor (eV)} \leq \frac{1240}{(\text{Wavelength (nm)})} \quad (2)$$

### 2.3. Photocatalytic activity measurements

The examination on the effectiveness of the B-TiO<sub>2</sub> was done by photocatalytic activity test, where the MB degradation performance was monitored with the help of light irradiation using 500 W xenon lamp. The suspension was prepared by mixing approximately 25 mg of photocatalyst in 100 ml of 15 mg/L (ppm) of MB aqueous solution and stirred in the absence of light for 60 mins. This preliminary step was done to ensure that the photocatalyst and the prepared substrate has reached an equilibrium state before irradiating it to light. After a fixed time interval, an aliquot of sample, approximately 2 ml was extracted from the photoreactor and centrifuged to get rid of nanoparticles. Subsequently, the supernatants were scanned with the UV-vis spectrophotometer (UV-2450, Shimadzu) between the wavelength of 800 nm and 200 nm. The concentration of MB was evaluated based on the maximum absorption band peak at around 668 nm. The concentration changes were described by  $C/C_0$ , where  $C_0$  and  $C$  is the initial concentration of MB and is the concentration of dye after reaction respectively. The MB degradation percentage ( $D_p$ ) was expressed in Eq. (3) as follows:

$$D_p = \left[ 1 - \left( \frac{C}{C_0} \right) \right] - 100\% \quad (3)$$

## 3. Catalyst Characterization

### 3.1. XRD

The changes in TiO<sub>2</sub> phase structure after boron doping were analyzed by XRD, as shown in figure 1.

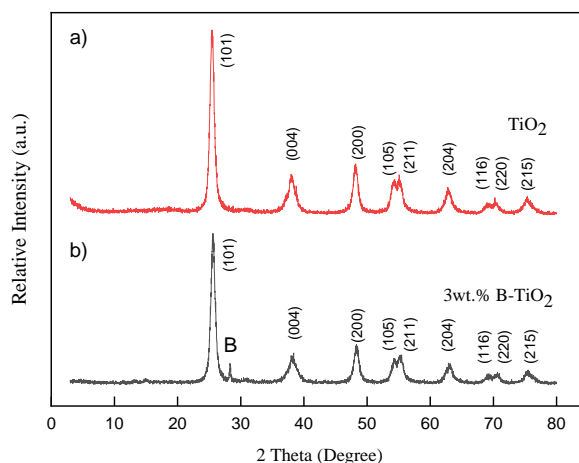


**Figure 1.** XRD patterns of the photocatalysts; (a) TiO<sub>2</sub> and (b) B-TiO<sub>2</sub> with B: boron B<sub>2</sub>O<sub>3</sub>/H<sub>3</sub>BO<sub>3</sub>.

The only crystalline phase identified in both catalysts is anatase, corresponding to (101), (004), (200), (105), (211), (204), (116), (220) and (215) crystal planes (JCPDS-21-1272). The appearance of sassolite boron structure (H<sub>3</sub>BO<sub>3</sub>) was also observed at the diffraction peak of  $2\theta = 28^\circ$  [12] for 3 wt.% B-TiO<sub>2</sub>. The anatase phase possess the advantage in the application of water treatment and water purification owing to its very photoactive property. There were no peaks associated with the other crystalline phases detected, suggesting a pure and single phase of produced TiO<sub>2</sub>. The intensity of anatase peak for doped TiO<sub>2</sub>, as depicted in figure 1, decreases as compared to as-synthesized TiO<sub>2</sub>. Through Scherrer's equation, the anatase crystallite size was determined as 10.12 nm and 10.04 nm for TiO<sub>2</sub> and 3 wt% B-

TiO<sub>2</sub> respectively. The introduction of boron precursor has confined the photocatalyst crystallite size. The similar effect was reported for the same catalyst and it was speculated that the anatase crystal growth was distorted by the presence of considerable amount of boron [12][13][14]. As a result, the surface area of doped TiO<sub>2</sub> may increase with the addition of boron compound [15].

### 3.2. UV-Vis Diffuse Reflectance Spectroscopy (DRS)

As compared to TiO<sub>2</sub> that exhibits an active activity on the UV-light region, the synthesized boron doped TiO<sub>2</sub> photocatalyst demonstrated a strong absorption for wavelength above 400 nm, indicating the visible light activity. See figure 2.

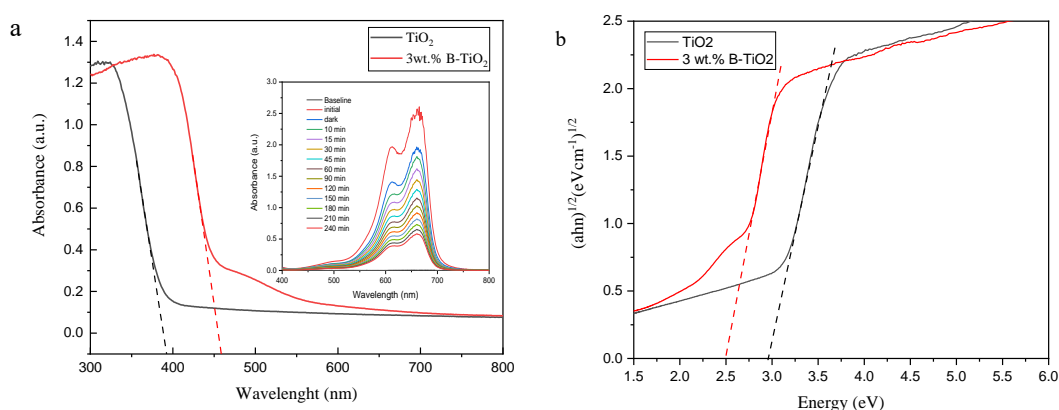


**Figure 2.** Diffusive reflectance UV-vis spectra (with inset of MB's spectra) and Tauc plot of the TiO<sub>2</sub> and 3wt.% B-TiO<sub>2</sub> photocatalysts

Starting from approximately 400 nm, absorption by TiO<sub>2</sub> drops towards the visible light region. Based on the spectral response in figure 2 (a), a plot of  $(\alpha h\nu)^{1/2}$  vs  $h\nu$  was developed as shown in figure 2 (b). The synthesized photocatalysts are assumed to be the indirect transition type ( $n = 1/2$ ) for the determination of the band gap energy. The determined band gaps are 2.96 and 2.50 eV for TiO<sub>2</sub> and 3 wt.% B-TiO<sub>2</sub>, respectively. The band gap energy of doped TiO<sub>2</sub> displays lower value than TiO<sub>2</sub> suggesting a shift in photonic absorption capability as a visible active photocatalyst.

### 3.3. Photocatalytic Study

Figure 3 displays  $\ln(C_0/C)$  against time, where  $C_0$  is the concentration of MB after 1 hour-absorption step at  $t = 0$  and  $C$  is the concentration at the irradiation time,  $t$ .

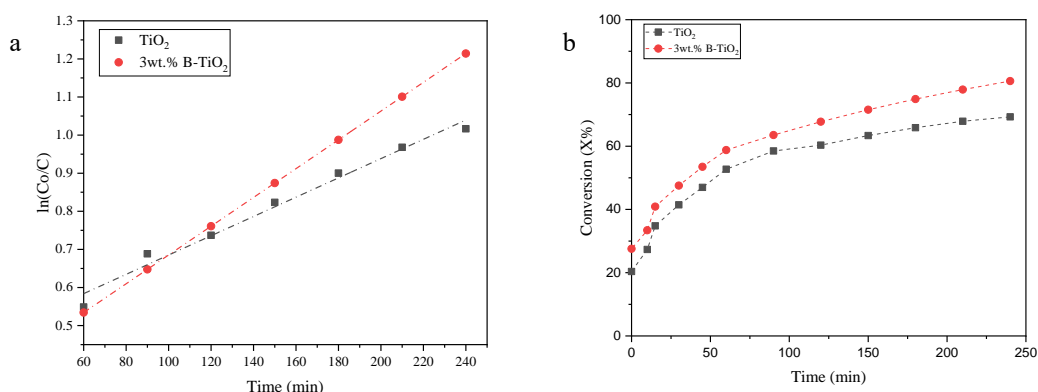
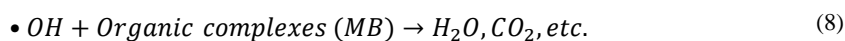
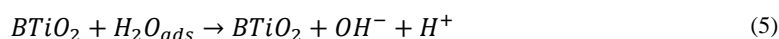
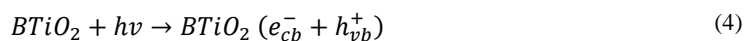


**Fig. 3.** Kinetic profiles of (a) concentration and b) conversion for MB decomposition with  $\text{TiO}_2$  and 3 wt% boron doped  $\text{TiO}_2$ .

The original concentration of the suspension is 15 mg/L. The catalytic effect of doped  $\text{TiO}_2$  on MB starts to show an obvious effect after the first 100 mins and becomes more apparent after 120 mins of the reaction, as indicated in figure 3 (a). The apparent specific reaction rate,  $k$  of doped  $\text{TiO}_2$  yielded a relatively higher value at  $3.78 \times 10^{-3} \text{ min}^{-1}$ , as compared to undoped  $\text{TiO}_2$  at  $2.53 \times 10^{-3} \text{ min}^{-1}$ . This led to the lower final concentration after 4 hrs of reaction. The higher conversion of MB by doped  $\text{TiO}_2$  may be caused by the lower band gap energy which improved the photon absorption during the irradiation of visible light source [16].

The highest conversion of MB is at 80.60 % with the photocatalyst loading of 0.25 g/L and the undoped  $\text{TiO}_2$  scored at 14 % lower in terms of conversion. This phenomena may be attributed to the limited generation of  $\bullet\text{OH}$  radicals produced between the hydroxide ions and photoinduced holes [17]. For both systems, the colour vanished from dark to light blue after 240 mins of irradiation were observed. The characteristic absorption was recorded at 668 nm, consistently throughout the entire course of the experiment. The MB absorbance reduced with the visible light exposure time, indicating an increase on the amount of dyes being degraded, see inset of figure 3 (a). Prior to irradiating the solution with the visible light, the system was allowed to reach equilibrium under the 1 hr of stirring. It was found that this pre-liminary step result in the reduction in absorbance at the maximum 24.5 %, depending on the initial dye concentration. The postulated mechanism of the studied system follows the concept of advanced oxidation process as shown below [16]:



The system is assumed to behave irreversibly. Applying the rate law model, together with the surface reaction limited (for single site), Langmuir-Hinshelwood model is used to describe the reaction behaviour:

$$-\frac{dC_A}{dt} = -r_A = \frac{kC_A}{1 + K_A C_A} \quad (9)$$

According to Eq. (9), the denominator can be simplified into ( $1 \gg K_A C_A$ )  $\sim 1$ . As a result, the MB degradation can be described by the Power Law model. For the pseudo first-order reaction kinetics, Eq. (9) can be simplified into:

$$-\frac{dC_A}{dt} = kC_A \quad (10)$$

The following expression is produced upon integration of Eq. (10) on both sides,

$$\ln \left( \frac{C_{A0}}{C_A} \right) = kt \quad (11)$$

Where  $C_{A0}$ ,  $C_A$ ,  $t$ ,  $k$  are initial concentration ( $\text{mgL}^{-1}$ ), concentration at time  $t$  ( $\text{mgL}^{-1}$ ), time (min), and apparent specific reaction rate ( $\text{min}^{-1}$ ) respectively. The specific reaction rate constant,  $k$  was determined from the slope of the linearized plot, constructed from the transient concentration data.

#### 4. Conclusion

A visible light active photocatalysts, B-TiO<sub>2</sub> were synthesized by sol-gel method. The photocatalytic activity of as-synthesized B-TiO<sub>2</sub> catalysts was evaluated by degrading MB under visible light irradiation. The incorporation of boron improved the photocatalytic activity of TiO<sub>2</sub> due to the narrower band gap and higher surface area with active sites for the photocatalytic reaction.

#### 5. References

- [1] Masudy P S, Siavash M R, Chua C, Kushwaha A, and Dalapati G K 2017 *ACS Appl. Mater. Interfaces* **9** 27596.
- [2] Takata T and Domen K 2019 *ACS Energy Lett.* **4** 542.
- [3] Tong H, Ouyang S, Bi Y, Umezawa N, Oshikiri N M, and Ye J 2012 *Adv. Mater.* **24** 229.
- [4] Kudo A and Miseki Y 2009 *Chem. Soc. Rev.* **38** 253.
- [5] Chong M N, Jin B, Chow C W K, and Saint C 2010 *Water Res.* **44** 2997.
- [6] Qi L, Yang Y, Zhang P, Le Y, Wang C, and Wu T 2019 *Appl. Surf. Sci.* **467** 792.
- [7] Wang X, Li Z, Shi J, and Yu Y 2014 *Chem. Rev.* **114** 9346–84.
- [8] Lee K, Mazare A, and Schmuki P 2014 *Chem. Rev.* **114** 9385–9454.
- [9] Liu C, Li X, Xu C, Wu Y, Hu X and Hou X 2020 *Ceram. Int.*, **46** 20943–53.
- [10] Yu J, Wang T, and Rtimi S 2019 *Appl. Catal. B Environ.* **254** 66–75.
- [11] Wei Y C and Lin C Y Y, 2015 *J. Manag. Organ.* **21** 755–771.
- [12] Fang B, Xing Y, Bonakdarpour A, Zhang S, and Wilkinson D P 2015 *ACS Sustain. Chem. Eng.* **3** 2381–88.
- [13] Rtimi S, Pulgarin C, Sanjines R, Nadtochenko V, Lavanchy J C, and Kiwi J 2015 *ACS Appl. Mater. Interfaces* **7** 12832–39.
- [14] Hao H, Shi J L, Xu H, Li X, and Lang X 2015 *Appl. Catal. B Environ.* **246** 149–155.
- [15] Su C Y, Wang L C, Liu W S, Wang C C, and Perng T P 2018 *ACS Appl. Mater. Interfaces* **10** 33287–95.
- [16] Quesada G M, Boscher N D, Carmalt C J, Parkin I P 2016 *ACS Appl. Mater. Interfaces* **8** 25024–9.
- [17] B. Wang B 2016 *ACS Appl. Mater. Interfaces* **8** 16009–15.
- [18] Shao J 2017 *Appl. Catal. B Environ.* **209** 311–9.
- [19] Patel N 2015 *J. Phys. Chem. C* **119** 18581–90.
- [20] Wang K 2019 *Appl. Catal. B Environ.* **250** 89–98.
- [21] Quiñones D H, Rey A, Álvarez P M, Beltrán F J, and Puma G L 2015 *Appl. Catal. B Environ.* **178** 74–81.

- [22] Bragg W L and Bragg W H 1913 *Proc. R. Soc. London. Ser. A, Contain. Pap. a Math. Phys. Character* **89** 248–277.
- [23] Kovac J D 1998 *J. Chem. Educ.* **75** 545.
- [24] Wade J 2005.
- [25] Zhang W 2013 *Talanta* **114** 261–267.
- [26] Zaleska A, Sobczak J W, Grabowska E, and Hupka J 2008 *Appl. Catal. B Environ.* **78** 92–100.
- [27] Chen D, Yang D, Wang Q, and Jiang Z 2006 *Ind. Eng. Chem. Res.* **45** 4110–4116.
- [28] Arifin M N, Karim K M R, Abdullah H, and Khan M R 2019 *Bull. Chem. React. Eng. & Catal.* **14** 219-27.
- [29] Cheng C K, Deraman M R, Ng K H, and Khan M R 2016 *J. Clean. Prod.* **112** 1128–35.

#### **Acknowledgement**

The authors would like to thank Universiti Malaysia Pahang for the financial support through internal grant RDU1803154.